Effects of Uncertainties in Component Fragilities on Lifeline Seismic Risk Analysis

Robin K. McGuire[1]

Abstract

Accurate calculation of the seismic risk for lifelines requires modeling the system as a function of its components, and requires accurate modeling of two engineering factors: (1) the spatial variability of earthquake ground motion including the ground motion correlation structure, and (2) the variability and correlation of component fragility functions. These conclusions are illustrated by evaluating the seismic performance of the Alameda, California, water distribution system for a range of earthquakes on the Hayward fault. A complete lifeline seismic risk analysis can account for the redundancy in a lifeline system design, but evaluating the benefits of that redundancy accurately requires modeling the correlation of responses of system components.

Introduction

The seismic risk analysis of an engineering lifeline is especially challenging because it involves multiple components, system performance under various conditions of damage or non-damage to its components, multiple earthquakes that might affect different parts of the system, and earthquake effects at multiple locations. A complete evaluation of risk to a lifeline must include a representation of: (a) the spatial extent of the engineering system, (b) the distribution of earthquakes in space and size, (c) the effects of earthquakes on system components, (d) the relationship between component damage and system performance, and (e) the probabilities associated with (a) through (d). Many studies have examined the individual elements above, and some have integrated these elements into a statement of losses or damage to lifelines and the associated probabilities.

[1]President, Risk Engineering Inc., 5255 Pine Ridge Road, Golden, CO 80403

This paper examines critical variables in the representation of component vulnerability to earthquake ground motion. Understanding the critical sensitivities is important in future research efforts to understand lifeline systems, their vulnerabilities to earthquakes, and ways to reduce that vulnerability through engineering analysis and lifeline design.

Methodology

To quantify the performance of a lifeline system, we define a set of mutually-exclusive, collective exhaustive system states that describe system performance. The earthquake risk to the lifeline is then the probability (typically, per year) that the lifeline is in a system state representing damage or loss. Mathematically this is calculated as:

$$\nu(\text{system state } i) = \sum_j \nu_j \int_m \int_x P[\text{system state } i \mid m, x]\ f_m(m) f_x(x) dm\ dx \qquad (1)$$

where ν is the annual rate of being in system state i, ν_j is the rate of earthquakes on fault j, $f_m(m)$ and $f_x(x)$ are probability distributions on magnitude and location for earthquakes on fault j, and $P[\text{system state } i|m, x]$ is the probability that the system is in state i given an earthquake of magnitude m at location x.

The probability of system state i given m and x can be calculated by assuming, without loss of generality, that (a) a system consists of a set of components, and (b) there is a deterministic relationship between the status of each component and the state of the system. The latter assumption could be generalized to a probabilistic relationship, but we have not found any system where, if one knows the status of all of the components, one cannot determine the state of the system. The probability of a system state i thus can be calculated as the probability that an earthquake occurs and causes the system components to reach a set of states such that the resulting system state is i.

In calculating the response of system components to an earthquake of magnitude m at location x, several variabilities may be important. First, the variability of ground motion amplitude A at each component location is generally large (typically a standard deviation of 60% to 100% of the mean when only the magnitude and distance of the earthquake and the general site geologic conditions are known). We represent this variability as:

$$\ln(A) = f(m, x) + \epsilon_a \qquad (2)$$

where

$$\epsilon_a = \epsilon_e + \epsilon_d + \epsilon_s + \epsilon_r \qquad (3)$$

In equation (3), the residual term ϵ (representing deviations from the mean value) is normally-distributed and is comprised of the sum of four components: an earthquake term ϵ_e, a directivity term ϵ_d, a site term ϵ_s, and a remaining error term ϵ_r. These represent, respectively, the component of ground motion variability contributed by the earthquake source, by directivity of energy from the source, by local soil conditions, and by remaining unknown factors

The advantage of representing variability in ground motion with equation (3) is that we can easily represent correlation in ground motion residuals between two sites. These correlations arise because the sites are affected by the same earthquake, they may be affected by similar directivity effects (if they are at similar azimuths), and they may be affected by similar soil effects (if they are close to one another). We represent the covariance $\gamma(h,k)$ of ground motion residuals at two sites h and k as:

$$\gamma(h,k) = \sigma_e^2 + 2\,\sigma_d^2 \cos\Theta_h \cos\Theta_k + \sigma_s^2 \exp[-(r(h,k)/r_o)^2] \quad (4)$$

where σ_e^2, σ_d^2, and σ_s^2 are the variances of residual terms ϵ_e, ϵ_d, and ϵ_s, respectively, Θ_h and Θ_k are the azimuths of sites h and k, with respect to the rupture, $r(h,k)$ is the distance between the two sites, and r_o is a standard correlation distance. The forms of the terms for directivity and for site effects are reasonable as first estimates of these effects. The factor of two in the directivity term ensures that, on average over all azimuths, the diagonal term in the covariance matrix equals the correct total variance of ground motion.

A second important factor in component responses is the variability in component fragility. We define the resistance B to ground shaking (in the same units as ground motion amplitude A) for each component using:

$$\ln(B) = Const. + \epsilon_b \quad (5)$$

where

$$\epsilon_b = \epsilon_m + \epsilon_u \quad (6)$$

In equation (5), ϵ_b represents the variation of components with respect to their resistance to ground shaking. This is calculated as the sum of ϵ_m, a variation that applies to all components simultaneously (it could represent, for example, the variation of a class of equipment supplied by one manufacturer), and ϵ_u, the residual variation. The correlation coefficient $\rho(i,j)$ of resistances between two components i and j can then be obtained as:

$$\rho(i,j) = \sigma_m^2/(\sigma_m^2 + \sigma_u^2) \quad (7)$$

In practice, one can group components by function or manufacturer, and represent the variation and correlation in each group as indicated in equations (5) through (7). This representation of variability and correlation allows us to examine the potential effects of these factors, in both ground motion and resistance, on calculated seismic risk for lifeline systems.

This formulation of lifeline seismic risk is similar to that of Taleb–Agha *et al.* (1975), Moghtaderizadeh *et al.* (1982), and Taylor *et al.*, (1985), in that random magnitudes and locations of earthquakes are considered as the causes of seismic risk, and an integration over all events is performed to calculate risk (probability of loss, damage, or lack of functionality) to the system. Our method is more general than the others, however, in that it handles variability in ground motion, correlation among ground motion residuals at different sites, random component responses (which is also a feature of Taleb–Agha *et al.*, 1975, and Taylor *et al.*, 1985) and correlation among component responses. The specific representation of the variabilities and correlations can be modified for specific applications, but the forms described above are adequate for a examining the influence of these factors on lifeline risk.

Application of the model is efficiently achieved by simulating a field of correlated ground motion values, one value at each site, rather than attempting an analytical solution. A set of ground motion values leads to a status for each component, from which the system state can be derived. Simulation of multiple fields of ground motions thereby allows the distribution of system states to be derived for that earthquake magnitude and location. Variabilities in earthquake magnitude and location (the two integrals in equation (1)) are easily treated with numerical integration.

Example Application

To investigate the effects of several parameters on lifeline risk, we apply equation (1) to an example problem. This is a pipeline network problem consisting of a water supply system in east San Francisco Bay (see Figure 1). This problem was first investigated by Moghtaderizadeh *et al.* (1982). The Hayward fault crosses the lifeline; the rate of seismic activity (magnitudes > 5) is 0.069 per year, the Richter b value is 0.8, and the maximum magnitude is 7.1 (These values are based on data presented by Wesnousky, 1986). Each magnitude M causes a rupture located at random on the fault of length $10^{(-3.31+0.708\ M)}$.

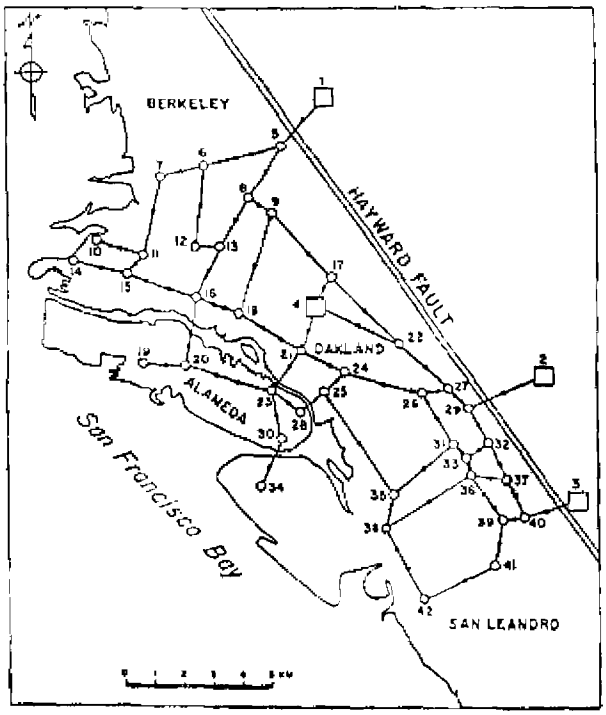

Figure 1: Water supply network in east San Francisco Bay (after Moghtaderizadeh, 1982).

Service to the island of Alameda is provided by three links (see Figure 1). Risk of total or partial loss of water service to Alameda was calculated using the link resistances and peak ground velocity (PGV) attenuation equation of Moghtaderizadeh *et al.* (1982). Four assumptions were considered on ground motion: (a) deterministic estimates, (b) random and independent residuals at each node, (c) random and perfectly-correlated residuals, and (d) random but correlated residuals. For all cases of random ground motion (except in Figure 5 below), $\sigma_{\ln\ PGV} = 0.5$ was used. For case (d), which is the most realistic representation of ground motion, 30% of the total variance was given to the first three factors in equation (3) and 10% was given to the last. For resistances, three

correlations were considered (perfectly correlated resistances, independent resistances, and a correlation coefficient of 0.5), along with three levels of variability: $\sigma_{\ln\ R} = 0.0$, 0.35, and 0.5.

Figure 2 illustrates the annual risk of failing one, two, or three pipelines to Alameda for the four representations of ground motion. (For this calculation the variability of resistance was taken to be zero.) Note that the ordinate on Figure 2 is annual probability of *occurrence*, not *exceedance*. It is clear that a deterministic representation of ground motion underestimates the risk; for this example, treatment of ground motion spatial correlation is also critical (for one or two failures); but this is not a general result. In terms of annual probability that one *or more* pipelines fail, the cases with random ground motion indicate a risk of about 0.025, and the deterministic case is 20% of this (i.e. it underestimates the risk by a factor of 5).

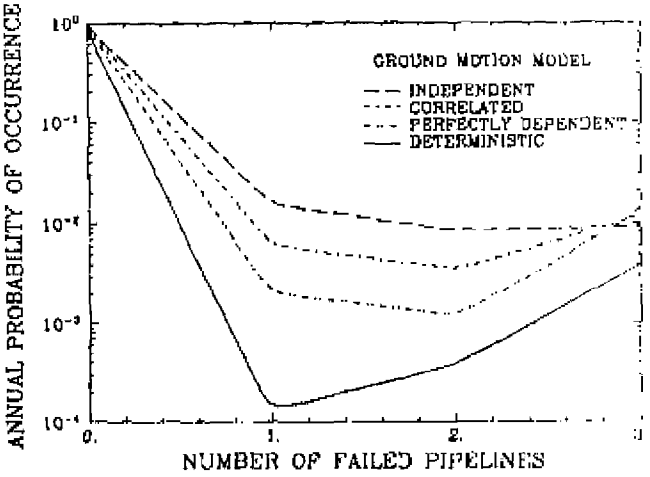

Figure 2: Risk of loss of service to Alameda; Sensitivity to ground motion model assumptions.

Figures 3 and 4 illustrate the sensitivity of results to the correlation among component resistances, for $\sigma_{\ln\ R} = 0.35$ and 0.5, respectively. In the former case we observe only moderate sensitivity to the correlation for some damage measures (i.e. for the failure of 2 pipelines in Figure 3 but not for the failure of 1 or 3), primarily because the variance in ground motion is twice as large as the variance in resistance. Thus the precise way in which resistance variability is modeled, in particular the correlation structure among components, is not critical. In Figure 4 the variance of re-

sistance is equal to that of the ground motion, and we find that the treatment of component resistance correlation is important for the failure of 1 or 2 pipelines but not for 3.

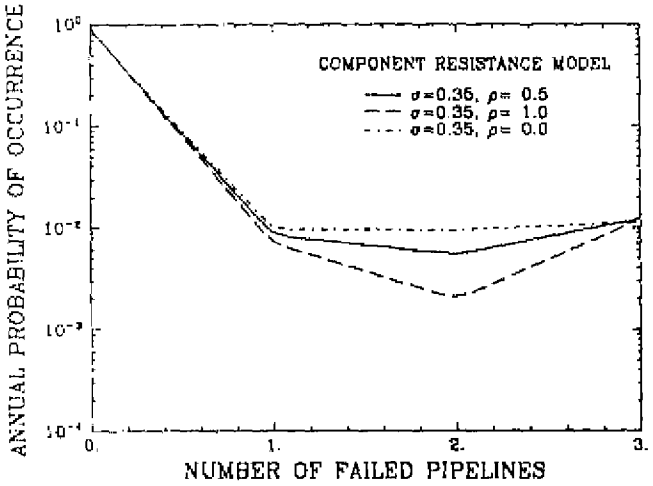

Figure 3: Risk of loss of service to Alameda; Sensitivity to ρ in component resistance model with $\sigma_{\ln,\ PGV} = 0.50$.

Figure 5 shows results for the case when $\sigma_{\ln,\ PGV} = 0.25$ and $\sigma_{\ln,\ R} = 0.5$, i.e. the variance of the ground motion is one-fourth that of the component resistances. In this case we see the expected result that the correlation structure of the component resistances is even more critical, i.e. when uncertainty in component response is large relative to uncertainty in ground motion, the correlation of resistance among components is important.

Conclusions

A complete seismic risk analysis of a lifeline system allows us to examine the sensitivity of results to models of variability and correlation of ground motion and component resistances. When the uncertainty in ground motion is large relative to uncertainty in component resistances to earthquake shaking, the model of spatial correlation for the ground motion affects the calculated seismic resistance to an important degree. When the uncertainty in resistance is large, the correlation of resistance among system components is important. These conclusions apply to detailed measures of seismic performance, specifically to whether 1 or 2 pipelines fail in the example lifeline analyzed here. In all cases the calculated probability of failure of all pipelines was surprisingly stable,

around 10^{-2} per year, regardless of models of uncertainty or correlation. This is just the probability that a large earthquake ($M \approx 7$) occurs close to the pipeline network, generating large ground motions and failing all three pipelines. The details of the uncertainty and correlation structure are irrelevant in this case. These conclusions are, of course, tentative; they should be confirmed with different lifelines and multiple performance measures.

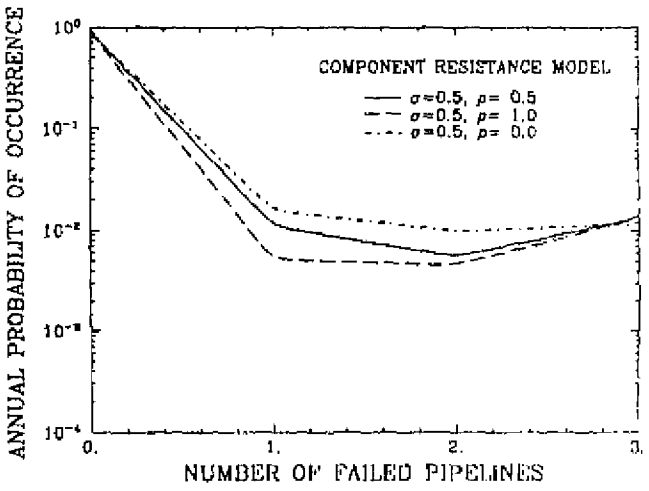

Figure 4: Risk of loss of service to Alameda; Sensitivity to ρ in component resistance model with $\sigma_{\ln\ PGV} = 0.50$.

References

1. Moghtaderizadeh, M., Wood, R.K., Der Kiureghian, A., and Barlow, R.E., "Seismic Reliability of Lifeline Networks," Jour. Tech. Counc., Amer. Soc. Civil Eng., 108, TC1, 60-78, (1982).

2. Taleb–Agha, Ghiath, and Whitman, R.V., "Seismic Risk Analysis of Discrete Systems", MIT, Department of Civil Engineering, MIT-CE R75-48, 72 p. (1975).

3. Taylor, C.E., Legg, M.R., Haber, J.M., and Wiggins, J.H., "New Lifeline Multiscenario Seismic Risk Techniques with a Model Application," Civ. Engrg. Syst., 2, 77-83, (1985).

4. Wesnousky, S.G., "Earthquakes, Quaternary Faults, and Seismic Hazard in California," Jour. Geoph. Res, 91, B12, 12587-12631, (1986).

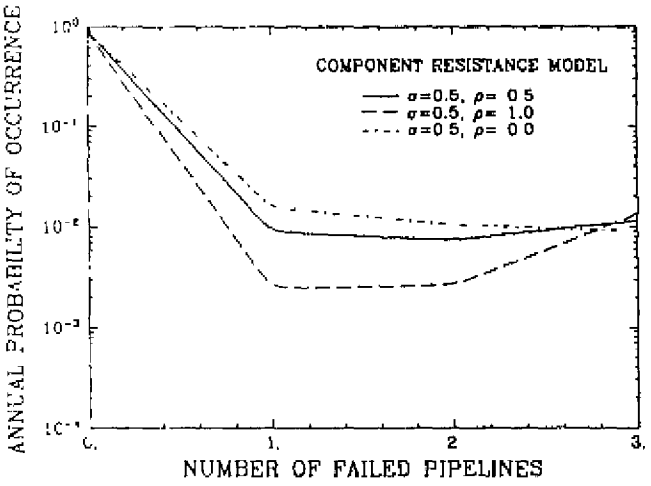

Figure 5: Risk of loss of service to Alameda; Sensitivity to ρ in component resistance model with $\sigma_{\ln\ PGV} = 0.25$.

PROBABILISTIC PREDICTION OF LOSSES TO LIFELINE SYSTEMS DUE TO EARTHQUAKES

Masoud Moghtaderi-Zadeh[1], Associate Member, ASCE

Abstract

An efficient and practical method for earthquake loss estimation for lifelines is developed, using the recent advances made in the areas of lifeline earthquake engineering and probabilistic seismic risk and structural response analysis. Recently developed loss algorithms and cost estimates for various types of lifeline components are used here to compute probabilities of exceedance of loss levels during a given time interval. A computer program for earthquake loss analysis of lifelines is developed. The use of the results of such an analysis by engineers and planners is demonstrated through an illustrative example

Introduction

Lifelines, such as gas or water distribution systems, communication networks, or transportation systems in large urban areas, are essential for the well-being of urban communities. Lifelines are complex systems and typically consist of a large number of sub-systems inter-connected physically and/or functionally and located throughout a vast area. Lifelines are expensive systems to design, construct, manage, retrofit, upgrade or replace Because of lifelines importance, high costs, complexity, and physical distribution, proper prediction of their performance against natural environmental hazards, such as earthquakes, has become an important challenge to overcome. The role and importance of lifelines becomes even greater when they are located in seismic regions. Performance of a lifeline immediately after a major earthquake is particularly vital for a community, because of the emergency services that are usually required following such events. Two examples of the importance of

[1]Lead Senior Engineer, ABB Impell Corporation, 5000 Executive Parkway, San Ramon, CA 94583.

lifelines in a seismic region are related to the occurrence of two major earthquakes (1906 and 1989) in the San Francisco Bay Area. As a consequence of the loss of the water distribution system in the San Francisco earthquake of 1906, fire destroyed a large section of the city. Most of the loss, as a result of the Loma Prieta earthquake of 1989, was due to damage to the lifeline systems in the Bay Area, especially to the transportation systems.

The results of an efficient and practical prediction of the performance of lifelines can be used by both the government sector (e.g., federal, state, county and city officials) as well as the private sector (e.g., insurance companies and utility owners). The results may be used in a number of areas such as in planning for emergency response, inventory, or local land use, estimating economic losses, estimating loss of lives, prioritizing funds, investigating the effects of alternative mitigation schemes, and in supporting management decision making processes.

The prediction of performance of lifelines against earthquakes may be with respect to the reliability of the systems, i.e., estimation of the probability of continuous functioning of the lifelines as intended, or it may be with respect to the losses, i.e., estimation of the probability of economic loss or loss of life. The reliability of lifelines has been investigated in the last two decades, e.g., Taleb-Agha, 1977 [11]; Moghtaderi-Zadeh et al., 1982 [9]; Shinozuka et al., 1981 [10]; Kiremidjian, 1980 [4]; and Eguchi et al., 1983 [3]. This paper addresses the latter aspect of the prediction of performance of lifelines, i.e., loss estimation, and only with respect to the economic losses. Thus, from this point forward the word loss is defined as an economic loss.

Broadly speaking, the economic losses can have two components: direct (primary) and indirect (secondary) losses. Direct losses include cost of repair or replacement of damaged components; e.g., replacement costs of a damaged main water pipe in a water distribution system. Indirect losses include user's costs and loss of revenue; e.g., loss of a facility from fire during or after an earthquake due to unavailability of water in a damaged main water pipe. This paper concentrates on direct losses only. Indirect and direct losses together will be considered in future studies.

This paper presents an efficient and practical method for predicting performance of lifelines against earthquakes. Based on the method a computer program is developed to compute the probabilities of of exceedance of loss to a lifeline system above threshold levels during prescribed time intervals. The computer program is then used to demonstrate the applicability of the methods to real life situations and

the usefulness of the results in supporting engineering and planning decision making processes.

Basic Formulation

Following the modern concepts of risk and reliability analysis, the performance of a system with respect to a predefined criterion, such as exceedance of a response quantity or total loss from a threshold level, can be formulated by a *Limit State Function* defined as

$$g(X) = g(X_1, X_2, \ldots, X_n) \tag{1}$$

in which X are random variables representing uncertain and time-invariant variables influencing the performance of the system and n is the number of the random variables. The case when the performance of the system is also influenced by stochastic processes representing uncertain and time-variant variables, is not discussed here. The limit state function g(X) is formulated for convenience such that for any given set of variables $x = (x_1, x_2, \ldots x_n)$, $\{g(x) < 0\}$ implies that the system does not satisfy the performance criterion and $\{g(x) > 0\}$ implies that the system satisfies the performance criterion (Throughout this paper upper case letters represent random variables and lower case letters represent specific values, except otherwise stated). The probability that the system does not satisfy the performance criterion, is then

$$P_f = \int_{\{g(x)<0\}} f_X(x)\, dx \tag{2}$$

in which $f_X(x)$ is the joint probability density function of X.

The methods to compute the above n-fold integration are grouped into: 1) direct integration (analytical and numerical); 2) simulation; and 3) first-order reliability methods (FORM). In general, it is impractical to compute the probability P_f by direct analytical integration except for trivial cases. For a small number of random variables and a simple domain of integration, it is practical and can be efficient to compute P_f by direct numerical integration. Simulation techniques can be used for most of the situations, however, they can become impractical when probabilities are very small (i.e., a large number of simulations is needed). The FORM, e.g., Madsen et al., 1985 [6], can be used for the computation of probabilities. The application of these methods to the probabilistic seismic hazard and performance evaluation of systems and lifelines can be found in, e.g., Reference [9] for direct integration; [10] for simulation; and Moghtaderi-Zadeh and Diamantidis, 1986 [8] for FORM. In this paper, direct numerical integration has been used to predict performance of lifelines.

Lifeline Performance Analysis

The probability that the losses, L , to a lifeline system during a given time interval of (0,t) due to the occurrence of earthquakes exceeds a prescribed threshold level, l, is given by

$$P_f(t) = \{L(X) > l, \text{ in time interval } (0,t)\} \quad (3)$$

where the vector X represents random variables influencing the losses to the lifeline , e.g., cost of repair or replacement of damaged components, and the number, magnitude and location of earthquakes occurring in the vicinity of the lifeline system. Defining the limit state function as

$$g(X) = l - L(X) \quad (4)$$

the problem is transformed to the basic formulation given by Eqs. 1 and 2. Assuming independence in the time of occurrence of earthquakes, the Poisson model can be used. Thus, the probability of having N earthquake in a time period (0,t), P_N, equals

$$P_N = [\ (\nu t)^N \exp(-\nu t)\ ] / N! \quad (5)$$

where ν is the mean rate of earthquake occurrence in the region. This model has well known short-comings, as described in Lomnitz and Rosenblueth, 1976 [5]. Nevertheless, it is a very useful model for application because of its mathematical simplicity and availability of the required information for its use. From the Poisson model the exceedance probability in time interval (0,t) can be written as

$$P_f(t) = 1 - \exp[-\nu t P_f] \quad (6)$$

in which P_f is the conditional probability of exceedance given one earthquake occurs in the region, i.e.,

$$P_f = \text{Prob}\ \{\ g(X) < 0, \text{ given one earthquake }\} \quad (7)$$

Assuming spatial independence of earthquake occurrences and using the total probability theorem, P_f can be obtained from

$$P_f = \Sigma(\nu_k/\nu)\, P_{fk} \quad (8)$$

where the summation is over all possible seismic sources in the region, ν_k is the mean rate of occurrence of earthquakes in source k, and P_{fk} is

$$P_{fk} = \text{Prob. } [\, g(X) < 0, \text{ given one earthquake occurs in source k }] \quad (9)$$

The probability P_{fk} can be computed in the following way.

Modeling of The Seismic Region

The fault-rupture model Der Kiureghian and Ang, 1977 [2] or its improved model which takes into account the width of the rupture area and the fault dip angle [8], can be used to model the seismicity in the region. The region is typically modeled through a set of three types of seismic sources. A *type-1 source*, namely a well-defined fault, is a fault plane with known location and orientation. A *type-2 source* is an area with known fault orientation but unknown fault locations. A *type-3 source* is an area with unknown fault locations and orientations. Figure 1 shows an example of a type-1 source, in which the location of the fault plane, i.e., the locations of its end points with respect to a coordinate system are known.

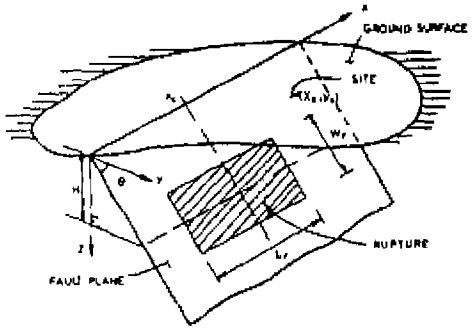

Figure 1 - Model for a type-1 seismic source

For each seismic source, earthquake magnitudes at various occurrences are assumed to be statistically independent and identically distributed random variables having probability density function, $f_M(m)$. Based on the Gutenberg-Richter magnitude recurrence relation, the probability density function of the earthquake magnitude may be written as

$$f_M(m) = [\beta \exp[-\beta(m-m_0)]] / [1-\exp[-\beta(m_u-m_0)]] \quad (10)$$

for $m_0 \le m \le m_u$, and zero, otherwise. β is the source seismicity parameter, m_u is the upper bound magnitude earthquake that the source is capable of generating, and m_0 is the lowest magnitude of engineering interest. An alternative representation of magnitude distribution is through its probability mass function, which is simply a table of magnitude ranges with their associated probabilities of occurrence.

Potential earthquake foci are assumed to be located on the fault plane at a random depth, H. In [8] it is shown how from the area and the length of the ruptured zone the width of the ruptured zone can be obtained for various configuration of the ruptured area. The width of the ruptured zone may affect the closest distance from a site to the ruptured area for dipped fault planes, Fig. 1. For each seismic source, the ruptured length, L_r, is assumed to be a function only of earthquake magnitude M as

$$L_r = 10^{(a_r+b_rM)} \quad (11)$$

The location of the rupture in each source is also random. For a type-1 seismic source, the rupture location on the fault plane, represented here by rupture midpoint location X_c , Fig. 1, a uniform distribution is considered. Other distributions can be also considered, if supported by sufficient data and justification. For the uniform distribution, assuming that rupture ends are confined within the fault ends, the probability density function for X_c is

$$f_{X_c}(x) = 1 / (L_f - L_r) \quad (12)$$

for $L_r/2 < x < L_f - L_r/2$, and 0 otherwise, where L_f is the fault length.

For a type-2 seismic source, the source can be divided into a finite number of imaginary type-1 sub-sources, with the imaginary fault orientations in the direction of the preferred orientation. The rate of occurrence of earthquakes in each sub-source can be assumed to be proportional to the contributory area of the sub-source. Therefore, the distribution of the location of rupture midpoint for each sub-source will be similar to that of a type-1 source, Eq. 12, with the L_f being the fault length of the imaginary fault.

For a type-3 seismic source, the source can be divided into a finite number of sub-sources. The rate of occurrence of earthquakes in each sub-source can be assumed to be proportional to area of the sub-

source. The location of the rupture midpoint in each sub-source is then assumed to be deterministic and at the geometrical center of the sub-source. The rupture length can be assumed to be negligible. However, if the rupture length can not be assumed to be negligible, then the orientation of the rupture can be accounted for in two ways. First, the orientation can be assumed to be uniformly distributed in the 0-π range, or it can be conservatively assumed to be in a direction which gives the minimum shortest distance to the sites of the components.

Modeling of Ground Motion Attenuation

Intensity of the ground motion at a site (e.g., peak horizontal acceleration (PHA), peak horizontal velocity (PHV) or Modified Mercalli Intensity (MMI)) due to an earthquake depends on many factors including the magnitude of the earthquake, the closest distance of the site from the rupture zone, the frequency content of earthquake waves arriving at the site, the intervening geology between the source and the site, and the site soil conditions. The attenuation of ground motion intensity, Y, with magnitude and distance can, in its general form, be written as

$$Y = \hat{Y}(M,R,c_i) \tag{13}$$

in which, M is magnitude, R is the shortest distance to the ruptured zone, and c_i are parameters which depend on soil conditions and frequency content of the ground motion. Examples of ground motion attenuation laws are:

$$\text{Ln PHA} = c_1+c_2M+c_3\text{Ln}[R+c_4\exp(c_5M)]+c_6R+c_7S_1 \tag{14a}$$
$$\text{Ln PHV} = c_1+c_2M+c_3\text{Ln}[R+c_4\exp(c_5M)]+c_6R+c_7\tanh(c_8D) \tag{14b}$$
$$\text{Log}_{10}\text{ PHA} = c_1+c_2I+c_3S_2 \tag{14c}$$
$$\text{Log}_{10}\text{ PHV} = c_1+c_2I+c_3S_2 \tag{14d}$$

where S_1 is a site factor representing shallow soils (S_1=0 for sites with more than 10 0 meters of soil overlying rock and S_1=1 otherwise), S_2 is a site term representing either alluvium (S_2=0), intermediate rock (S_2=1), or basement rock (S_2=2), and D is the depth to basement rock. The coefficients c_i, which are different for each of the above equations, are given in [1].

Modeling of Lifeline System

A lifeline is usually modeled as a network of interconnected nodes and links, referred to as components. As a result of an earthquake, a component may be in any number of states between the two states of no damage and complete damage. Depending on the level

of damage to the component, the costs incurred may vary from zero to a full replacement cost which consists of costs of cleaning and removal of the damaged component and costs of design, construction, and installation of a replacement for the component. The losses to a component can be given in terms of a percentage of the component total replacement costs, R_c.

The losses to a component can be related to one or more intensities of ground motion at the site of the component. In its simplest form the level of damage may be stated as a function of one ground motion intensity level at the site, e.g. MMI. These functions are usually referred to as component *Loss Algorithms*, In [1] simple yet practical loss algorithms for various types of components of a water distribution system are given. Figures. 3-6 show examples of loss algorithm for the water distribution system. For example, for an unreinforced masonry pumping station with a replacement cost of R_c = \$156,000, the loss due to earthquake shaking is given by

$$L = 0.0 \quad \text{for } I<7.08 \tag{15a}$$
$$L = (-1.77 + 0.25I)R_c \quad \text{for } 7.08<I<9 \tag{15b}$$
$$L = (-3.03 + 0.39I)R_c \quad \text{for } 9<I<10.33 \tag{15c}$$
$$L = 1.0\,R_c \quad \text{for } 9<I \tag{15d}$$

in which, I is MMI at the site of the pumping station.

When computing losses to a component of a lifeline system, the damage to the component due to various attributes of the earthquake should be considered. The most common causes of damage to lifeline components due to earthquake are: 1) ground shaking; 2) liquefaction; 3) ground differential movement (surface rupture); 4) soil settlement and compaction; 5) land slides; and 6) flooding (tsunami, seiche). The loss algorithms for each attribute of earthquake induced damage may be different. In [1], it is shown how to incorporate the effect of liquefaction induced damage in the analysis. Simply stated, the effect of liquefaction can be given as an expected loss to components located in susceptible liquefaction zones as:

$$L = P_{liq}L_{liq} + (1-P_{liq})L_{shk} \tag{16}$$

in which P_{liq} is the probability of liquefaction at the site of the component, L_{liq} is the loss to the component if liquefaction occurs, and L_{shk} is the loss to the component if liquefaction does not occur.

Total Losses

The total loss to a lifeline system is simply the sum of the all losses to the individual component and is given by

$$L = \sum L_i \tag{17}$$

where the summation is over all components of the lifeline and L_i is the loss to the i-th component.

Thus the probability that total loss to a lifeline system exceeds a threshold level l, given one earthquake occurs in source k , Eq. 9, can be obtained from

$$P_{l,k} = \int\int I(x,m,k)\, f_{X_k}(x,m,k)dx\, f_M(m,k)dm \tag{18}$$

where the indicator function, $I(x,m,k)$ for a given earthquake with magnitude m located at x within seismic source k, is defined equal to 1.0 when $L>l$, and 0 when $L<l$

Computation of Loss Probability

Based on the above formulation a computer program has been developed to compute loss probabilities. The earthquake loss analysis for lifelines (ELAL) computer program, written in FORTRAN language, is an efficient program for the computation of loss probabilities. On a 1180 VAX computer, the typical CPU time is about 10 seconds, for the computation of losses to a lifeline system of 18 nodes and 50 links, located in a seismic region represented by a background seismicity source of type-3 and three type-1 sources.

Illustrative Example

The hypothetical water distribution system given in [1] is simplified and used here for illustration of the methodology. The system consists of 18 node-components and 19 link-components, Fig. 2. In this paper only the node-components are considered. Table 1 contains the required information on each node-component of the hypothetical water distribution system. The loss algorithms referred to in Table 1 are shown in Figs. 3-6.

Figure 7 outlines the seismic sources in the vicinity of the water distribution system. The system is located within the near field of a blind thrust fault, modeled as two type-1 seismic sources here

(seismic source 2&3). A second major fault system, a strike-slip fault, in the region is also modeled as a type-1 seismic source (seismic source 1). Since all the potentially damaging fault systems have not been identified, a background source is considered and modeled as a type-3 seismic source (seismic source 4). Table 2 gives the characteristics of the modeled seismic sources. It is assumed that all the fault planes are vertical and that the upper part of a ruptured zone reaches to about a depth of 2 km for all earthquakes on these sources. The distribution of earthquake magnitudes for each seismic source is given in Table 3. The rupture length for seismic source 1,2 and 3 is calculated from Eq. 11, with $a_r = -2.77$ and $b_r = 0.62$, with the length being in km [1].

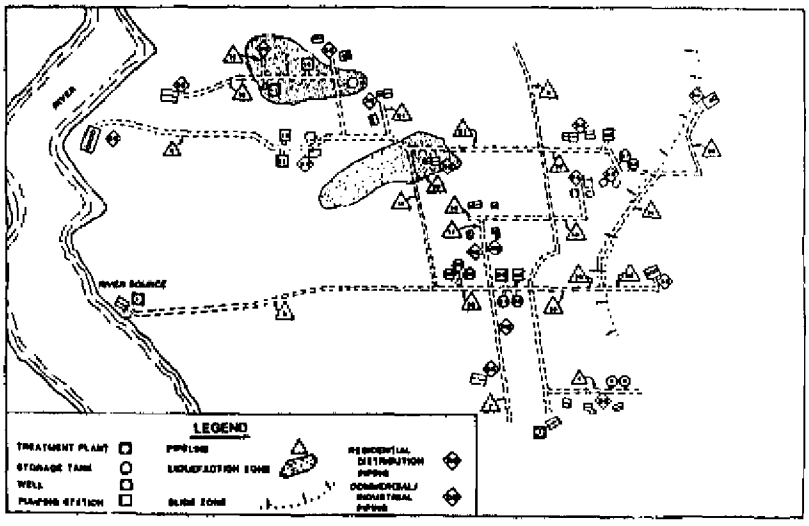

Figure 2 - Hypothetical Water Distribution System

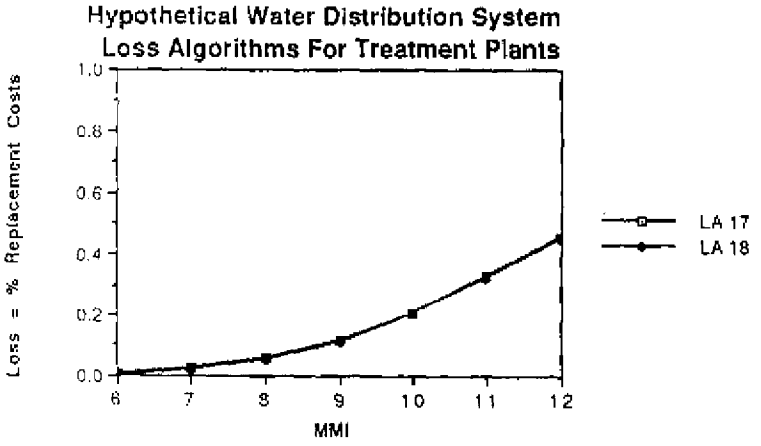

Figure 3 - Loss algorithms for the two treatment plants

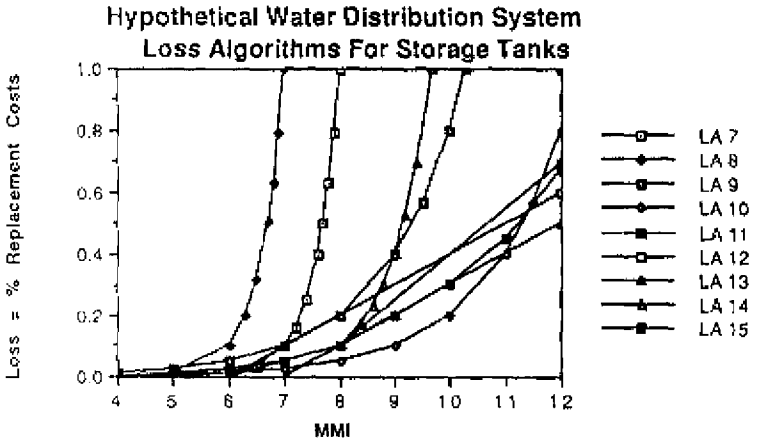

Figure 4 - Loss algorithms for the nine storage tanks

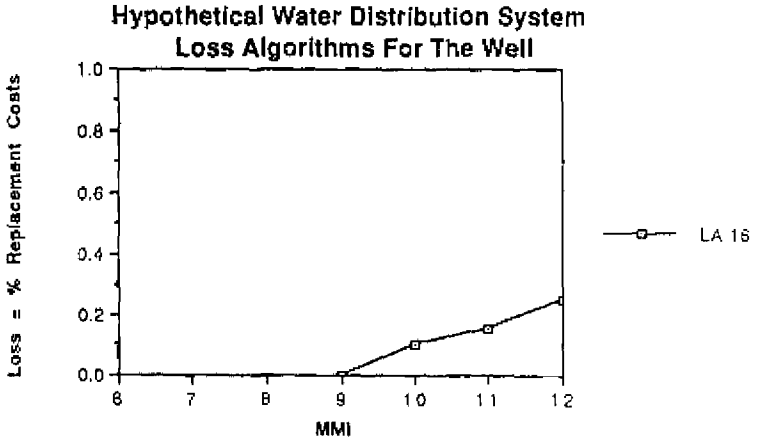

Figure 5 - Loss algorithm for the well

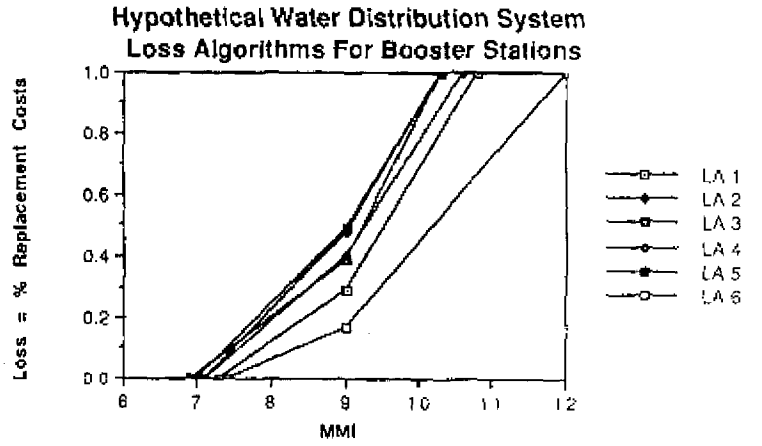

Figure 6 - Loss algorithms for the six pumping stations

Table 1 - Node-Components of the Hypothetical Water Distribution System

ID (1)	Facility Type (2)	X-coord (3)	Y-coord (3)	Depth (4)	Replace. Costs (5)	LA (6)
1	Treat. Plant	-1.0	5.0	4.2	8,426,000	17
2	Treat. Plant	7.0	-1.0	2.0	20,842,000	18
5	Strg Tank	9.0	2.0	2.0	580,000	7
6	Strg. Tank	9.0	2.0	2.0	580,000	8
25	Strg. Tank	5.5	6.0	3.5	645,000	9
26	Strg. Tank	5.5	6.0	3.5	645,000	10
27	Strg. Tank	5.5	6.0	3.5	975,000	11
31	Strg Tank	6.5	6.0	3.2	1,900,000	12
32	Strg Tank	6.5	6.0	3.2	1,900,000	13
37	Strg Tank	10.0	10.0	3.0	1,040,000	14
38	Strg Tank	10.0	10.0	3.0	1,040,000	15
11	Well	1.0	13.0	5.5	381,456	16
13	Booster Stn	2.0	10.5	5.0	376,100	1
14	Booster Stn.	2.0	10.5	5.0	375,100	2
16	Booster Stn.	2.7	13.0	5.0	175,000	3
29	Booster Stn.	6.5	6.0	3.2	156,000	4
30	Booster Stn.	6.5	6.0	3.2	156,000	5
36	Booster Stn	10.0	11.0	3.5	193,000	6

Notes.

(1) Node identification number, Fig. 2.

(2) Components are grouped together according to their use. However, there are differences in, e.g., construction material, age, and capacity, components within each group.

(3) Coordinates (in km) of location of the nods with respect to the referenced coordinate system, Fig. 7.

(4) Depth (in km) to basement rock.

(5) Replacement costs (in $) of nodal components.

(6) Loss algorithm (LA) identification for each node, Figs. 3-6.

Table 2 - Description of Seismic Sources in the Region

ID (1)	Rate (2)	XI (3)	YI (3)	XJ (3)	YJ (3)	XK (3)	YK (3)	XL (3)	YL (3)
1	0.19	-6.0	78.0	56.0	-6.0	-	-	-	-
2	0.06	10.0	8.0	18.0	20.0	-	-	-	-
3	0.11	10.0	8.0	20.0	-16.0	-	-	-	-
4	0.46	-20.0	-20.0	60.0	-20.0	60.0	80.0	-20.0	80.0

Notes:

(1) Seismic source identification number.
(2) Mean annual rate of earthquakes on each source.
(3) Coordinates (in km) of location of the ends of the fault lines or vertices of the area sources with respect to the referenced coordinate system, Fig. 7.

Table 3 - Probability Distribution for Earthquake Magnitudes

Source 1		Source 2 & 3		Source 4	
M (1)	P (2)	M (1)	P (2)	M (1)	P (2)
6.70	0.657	5.50	0.730	5.25	0.600
7.30	0.217	6.10	0.243	5.75	0.240
7.80	0.126	6.70	0.020	6.25	0.160
	-	7.30	0.007	-	-

Notes:

(1) Earthquake magnitude level.
(2) Probability of occurrence.

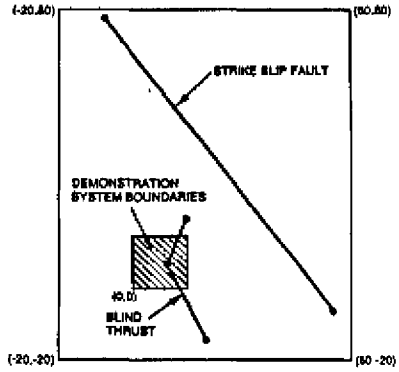

Figure 7 - Seismic sources in the region of the hypothetical system

Some of the main results of the analysis are plotted in Figs 8-16. Figures 8 and 9 demonstrate the contribution from each of the four seismic sources to the total loss distribution. Figure 8 compares the four sources when an earthquake occurs in each one of them. Clearly, source 1 has the most potential to damage the system if an earthquake occurs on it. In contrast source 4 has the least potential to damage the system when an earthquake occurs on it. However, taking into account the chance of occurrence of earthquake on each source, Fig. 9, demonstrates that source 4 contributes the most to potential losses to the system of up to about $50,000. The potential damages above $100,000, however, are almost all due to earthquakes on source 1. These and similar results can be used by engineers when upgrading the system against earthquakes.

Figures 10 and 11 illustrate the effect of earthquake magnitudes on the loss distribution. For an earthquake on source 4, as expected, the losses increase as the magnitude of earthquake becomes larger. In this case the maximum magnitude of 6.25 causes the highest damage. However, accounting for probability of occurrences, Fig. 11 demonstrate that, smaller but more frequent earthquakes of magnitude 5.25 contribute the most to the loss to the system. Again, these and similar results can be used by engineers for seismic retrofit of the system.

Figures 12-15 illustrate the total loss to the system according to each group of components. These figures give the loss distribution for each group conditioned on the occurrence of an earthquake in the region. Comparing Figs. 12-15, it is illustrated that the treatment plants, with ID = 1 & 2 in Table 1, are the most contributors to the losses to the system. This may have been expected, due to the fact that their replacement costs are about 4-100 times more than other components (even though the maximum loss to these components can reach only about 50% of their replacement costs, Fig. 3). On the other hand, the contribution of the well, ID = 11 in Table 1, to total loss is minimal as demonstrated by Fig. 14. These results can be used by planners, e.g, to decide which system should be upgraded and to what degree and how much should be invested in each system upgrading.

Figure 16 demonstrates the increase of loss probability as a function of the time interval for which the system is used. There are two implied assumptions underlying these figures. Firstly, it is assumed that when an earthquake occurs, the system will be repaired and brought to its original earthquake resistant levels immediately after the earthquake. Secondly, the system configuration, resistance to earthquake and component replacement costs do no change with time, which is not the case. However, as a tool for estimating the relative

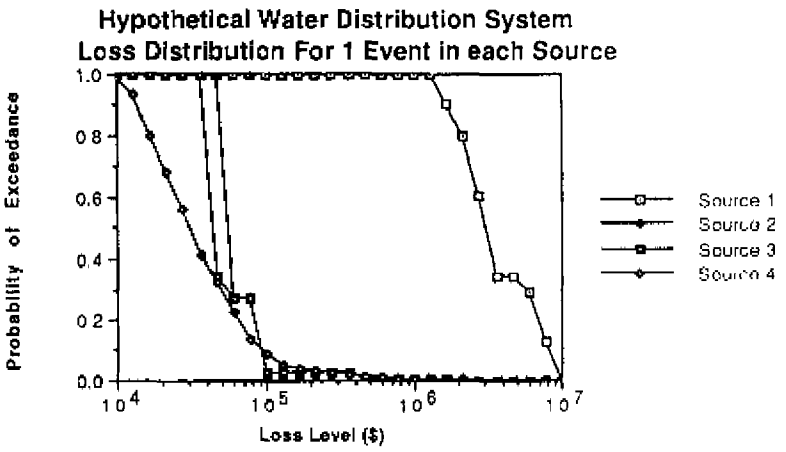

Figure 8 - Seismic source effects on loss distribution, conditioned on the occurrence of one earthquake in each source

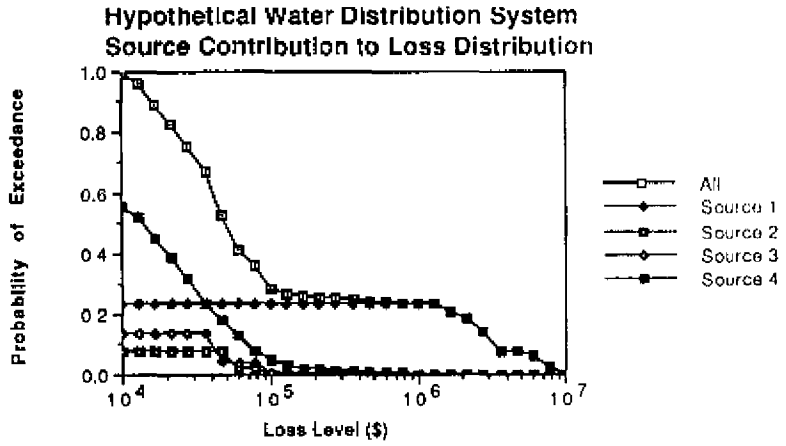

Figure 9 - Contribution of each seismic to loss distribution, conditioned on the occurrence of one earthquake in region

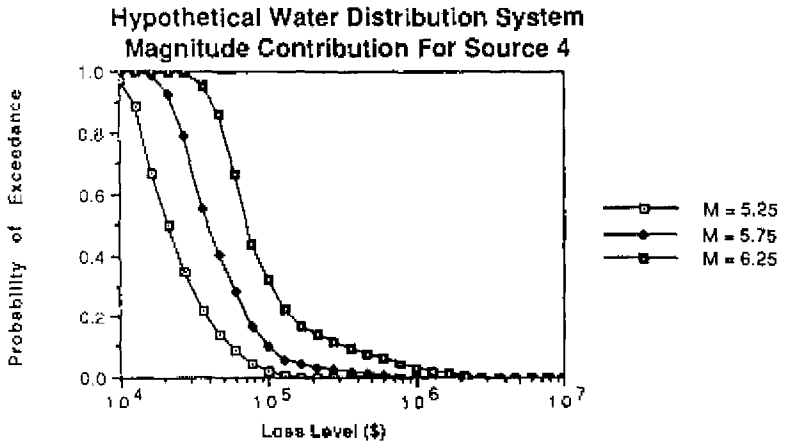

Figure 10 - Effect of earthquake magnitude of the loss distribution

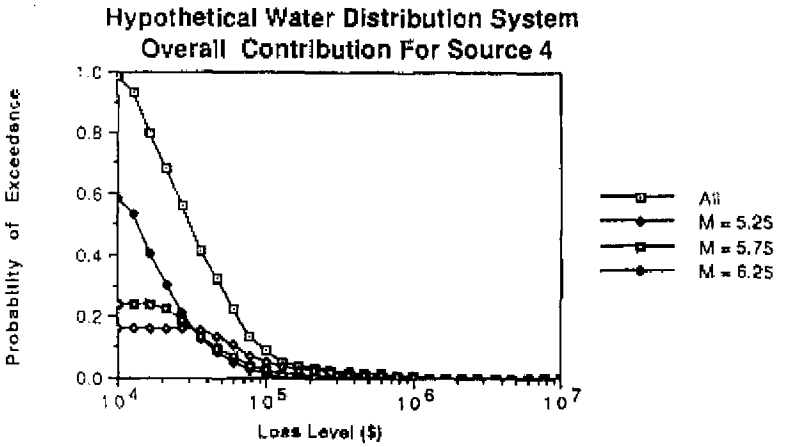

Figure 11 - Effect of earthquake magnitude on loss distribution, conditioned on the occurrence of one earthquake on source 4

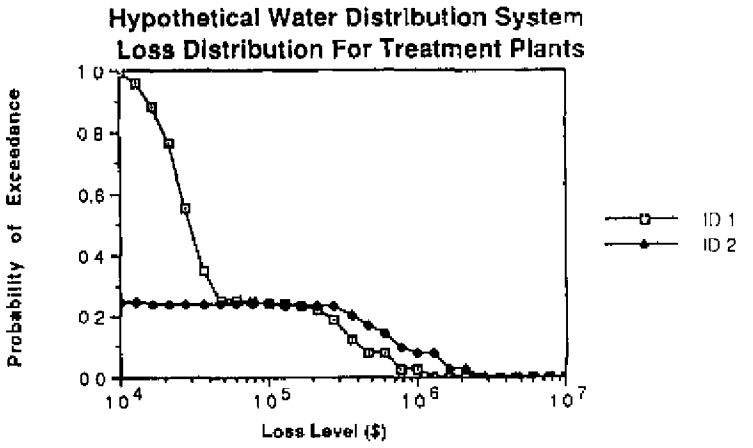

Figure 12 - Loss distribution for water treatment plants, conditioned on the occurrence of one earthquake in the region

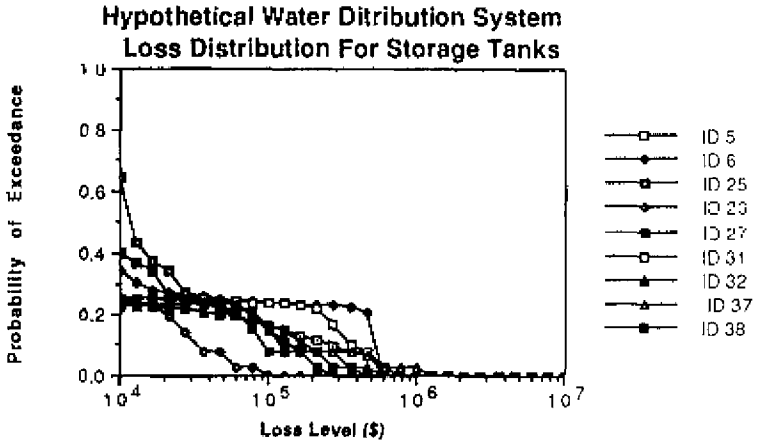

Figure 13 - Loss distribution for water storage tanks, conditioned on the occurrence of one earthquake in the region

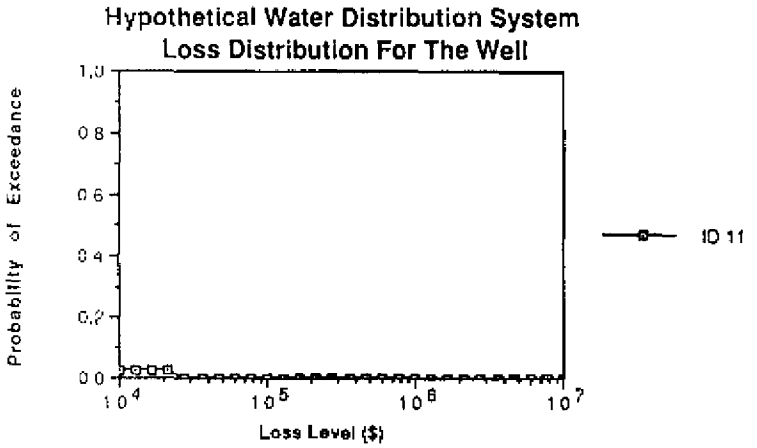

Figure 14 - Loss distribution for the well, conditioned on the occurrence of one earthquake in the region

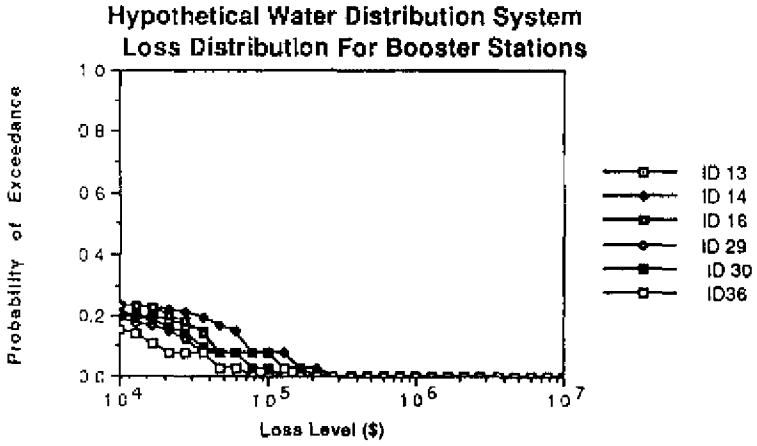

Figure 15 - Loss distribution for pumping stations, conditioned on the occurrence of one earthquake in the region

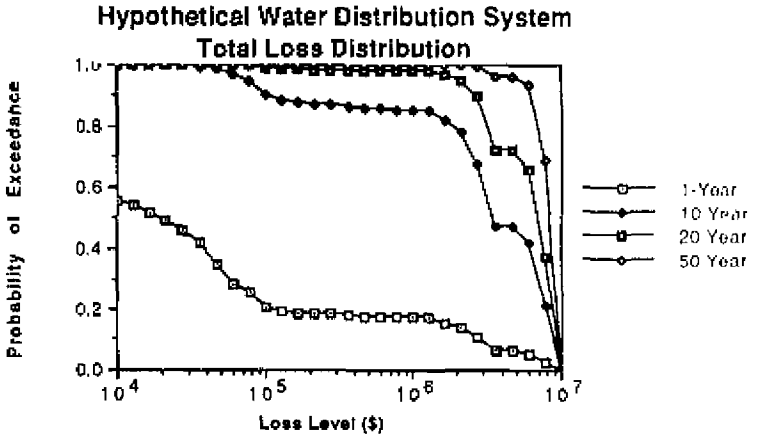

Figure 16 - Total Loss distribution for the system for various time intervals

losses in future, plots of Fig. 16 are very useful tools for planners, owners, and insurers.

Summary and Conclusions

This paper demonstrated a method for probabilistic prediction of losses to lifeline systems due to earthquakes. With the ever increasing dependence of urban areas on lifelines and ever increasing costs of design, construction, management, retrofit and upgrade of lifelines and ever increasing complexity of the lifeline systems, the importance and usefulness of such efficient and practical methods becomes evident. This paper presented the applicability of the method to real life lifeline systems and demonstrated the usefulness of the results through application to a hypothetical water distribution system. It is demonstrated here that for lifeline engineering and planning, especially with respect to earthquakes, lifelines must be treated as one whole system, not separate components.

For future research and work the following is suggested:

1. Consideration of both direct and indirect losses.
2. Demonstration and use of probabilistic loss estimation methods in the study of mitigation strategies.
3. Development of loss algorithms for components of lifelines other than water distribution systems.

Acknowledgement

Thanks are due to ABB Impell Corporation for the use of their computing facilities and support for the presentation of this paper. The opinions in this paper are those of the author and do not necessarily reflect those of ABB Impell Corporation.

Appendix I.--References

[1] Committees on Water and Sewage and Seismic Risk of the Technical Council on Lifeline Earthquake Engineering, 1991, "Seismic Loss Estimates for a Hypothetical Water System," To be published by ASCE.

[2] Der Kiureghian, A. and A. H-S. Ang, 1977, "A Fault Rupture Model for Seismic Risk Analysis," Bulletin of the Seismological Society of America, Vol. 64, No. 4, pp. 1173-1194, August.

[3] Eguchi, R.T., M.R. Legg, C.E. Taylor, L.L. Philipson, and J.H. Wiggins, 1983, "Earthquake Performance of Water and Gas Supply Systems," J.H. Wiggins Company Report No. 83-1396-5 for the National Science Foundation, Redondo Beach, CA.

[4] Kiremidjian, A.S., 1980, "Reliability of the California State Water Project, " ASME, the Pressure Vessels and Piping Division, the Century 2 Pressure Vessels and Piping Conference, August.

[5] Lomnitz, C., and E. Rosenblueth, (Editors), "Seismic Risk and Engineering Decisions," Elsevier, Amesterdam, Netherlands, 1976.

[6] Madsen, H.O., S. Krenk and N.C. Lind, "Methods of Structural Safety," Prentice-Hall, Englewood Cliffs, NJ, 1985.

[7] McGuire, R.K., 1988, "Seismic Risk for Lifeline Systems: Critical Variables and Sensitivities," Proceedings, 9th World Conference on Earthquake Engineering, Tokyo.

[8] Moghtaderi-Zadeh, M. and D. Diamantidis, 1986, "Full Probabilistic Seismic Risk Evaluation," Proceedings of the 8th European Conference on Earthquake Engineering, Vol. 1, Lisbon.

[9] Moghtaderi-Zadeh, M., R.K. Wood, A. Der Kiureghian, R.E Barlow, and T. Sato, 1982, "Seismic Reliability of Flow and Communication Networks," Journal of Technical Councils, American Society of Civil Engineers, Vol. 108, TC1, May.

[10] Shinozuka, M., Tan, R. Y., and Koike, T., 1981 "Serviceability of Water Transmission Systems under Seismic Risk," Proceedings, Second ASCE-TCLEE Specialty Conference on Lifeline Earthquake Engineering, Oakland, CA, August.

[11] Taleb-Agha, G., 1977, "Seismic Risk Analysis of Lifeline Networks," Bulletin of the Seismological Society of America, Vol. 67, No. 6, pp. 1625-1645.

[12] Taylor, C.E., M.R Legg, J.M. Haber, and J.H. Wiggins, 1985, "New Lifeline Multiscenario Seismic Risk Techniques with a Model Application," Civil Engineering Systems, Vol. 2, pp. 77-83, June.